Journal of Materials and Electronic Devices 2 (2025) 33-41

JOURNAL OF MATERIALS AND ELECTRONIC DEVICES

JMED

Investigation of the N-Si Dative Bond at the atomistic level in drug carrier/drug delivery nanosensor applications of Si-CNTs

Serap SENTURK DALGIC

Department of Physics, Faculty of Science, Trakya University, 22030 Edirne, Turkey

This study investigates the interaction of drug molecules with silicon-functionalized carbon nanotubes (Si-CNTs) through N→Si dative bonding, aiming to elucidate their potential in drug delivery and carrier systems. Quantum chemical analysis of N→Si bonds, based on bond length, electron density at bond critical points (ρ_{BCP}), Laplacian ($\nabla^2\rho$), and energy density parameters revealed varying bond strengths and characters across different drug–Si-CNT complexes. Most N→Si interactions exhibited weak to moderate dative character, suggesting transient binding suitable for controlled drug release in delivery applications. Notably, one complex of Imiquimod (IMQ)/Si-CNTs structures displayed a strong covalent-like dative bond, indicating its potential as a stable drug carrier. Findings from QTAIM, NCI, and RDG analyses underscore the key role of N→Si dative bonds in governing drug adsorption and release on Si-CNT platforms and demonstrate the usefulness of topological and energetic parameters for predicting drug–nanotube interactions. It may be suitable for both drug delivery and carrier systems. The N→Si coordinative bond is not only a fundamental bonding mode that controls the electronic and chemical properties of Si-CNTs; it is also a decisive theoretical element in targeted drug delivery, nanosensor design, and the rational design of functional carbon nanomaterials

Keywords: *Imiquimod (IMQ), N-Si dative bond, DFT, QTAIM, CNTs*
Submission Date: 15 September 2025
Acceptance Date: 25 November 2025

**Corresponding author:* dserap@yahoo.com, serapd@trakya.edu.tr
https://orcid.org/0000-0003-2541-9214

1. Introduction

In recent years, nanotechnology approaches have led to significant advances in the design and development of nano-sized intelligent systems for drug delivery or as drug carriers in the diagnosis and treatment of cancer. Some specific drug delivery systems (DDS) aim to target smart nanocarriers to cancer cells. Therefore, the chemical structure and detection capability of the drug carrier are important. Today, a wide variety of intelligent drug delivery systems include carbon fullerene, carbon nanotube (CNT), graphene, and gold nanoparticles, silica nanoparticles, and silver nanoparticles have been developed, and investigations in this area are rapidly advancing [1-3].

Smart or intelligent drug delivery systems can overcome the limitations of conventional drug delivery systems and enhance the effectiveness and safety of therapeutic drugs [3]. It is known as targeted or intelligent drug delivery, which offers control over release and reduces the frequency of dosing and toxicity. On the other hand, smart nanomaterials have been explored as drug carriers for the treatment of numerous conditions, including cancer. Carbon-based nanoparticles (NP), or carbon-based nanostructures, are well-known nanocarrier (NC) systems. Various types of NC are used for drug delivery in cancer therapy, e.t.c. The inorganic NCs, namely Graphene-based NCs, Nanoshells, Carbon Nanotubes (CNTs), silica NPs, and nanomaterials (NMs), are being used as transport modules for another substance, such as a drug [3].

In particular, silica-based nanoparticles (mesoporous silica nanoparticles) offer a promising platform for controlled drug loading and release due to their high surface area, tunable porosity, and surface-functionalizable chemical structures. Thus, silica nanoparticles are a specific class of smart nanoparticles with high drug carrying capacity, easy functionality and biocompatibility [4].

On the other hand, CNTs are considered nano-vehicles for delivering various therapeutic agents due to their high electrical conductivity and unique properties [5-19]. CNTs have also served as carriers of anticancer molecules such as gemcitabine (GEM), Aldara (ALD), Efafirnez [7-11].

It has been noted that metal-doped CNTs are of special interest in drug delivery and drug carriers [11-19]. Moreover, metal-doped CNTs or NPs also offer critical advantages, owing to their ability to be surface-engineered for specific purposes [7]. Some nanotubes' coordinated bonding ability helps the drug NC and drug delivery. Among them, Si-doped CNTs have received considerable attention in the literature [11-19]. The N-Si dative bond plays a significant role in this subject.

The N-Si dative bond has not been extensively investigated in specific DDS designs [3]; it plays an important role in the surface functionalisation of silica/silicon-based carriers (e.g., amine groups) [3]. N-Si dative (coordination) bonds are special types of bonds formed in organosilicon compounds when a nitrogen atom (N) donates two electrons to an empty silicon orbital, and are defined in pentacoordinate cilatran model systems [20-22]. These types of bonds can provide structural advantages in DDS design, such as surface modification and stabilisation of functional groups [3-5].

This work aims to provide a clear picture and understanding of the nature of interactions in the studied complexes, to apprehend the role of non-covalent interactions in the stability of the dative bonds, and to extend further the results obtained from the topology analysis of Quantum Theory of Atoms in Molecules (QTAIM) based on Bader's theory [23]. We investigate non-covalent interactions in the systems using the Non-Covalent Interaction (NCI) analysis [24] based on the reduced density gradient (RDG) procedure.

2. Materials and Methods

This study investigates the adsorption of the IMQ molecule on (6,0) Si-SWCNTs with a length of 10 Å, composed of 47 C and 12 H atoms (Si-C47H12), using DFT implemented in Gaussian 09W [25]. These complexes were created to compare the effect of the Si atom on drug adsorption in previous studies [11,14-16].

The optimisations of all geometric structures were carried out using the M062X functional along with the 6-31G(d) basis set. The M062X function with the/6-31G(d) method, used in recent studies [26,11,14-16], demonstrated that the M062X level in DFT calculations effectively models molecular interactions compared to other conventional functionals.

At the same time, M06-2X/6-31G(d) provides more reliable results for drug delivery applications by describing non-covalent and weak interactions [References in 11 and 14].

Frequency calculations were also performed using a similar level of theory to evaluate the stability of optimised structures and confirm that all stationary points represent minima on the potential energy surface.

The following equation calculates the adsorption energy of the IMQ drug:

$$E_{ads} = E_{complex} - \left(E_{IMQ} + E_{Si-CNT}\right) + E_{BSSE} \qquad (1)$$

where E_{IMQ}, and $E_{Si\text{-}CNT}$, $E_{complex}$ represent the energy of the IMQ, Si-CNT and complex, respectively. E_{BSSE} represents the Base set superposition error energy (BSSE) and was defined as an approximate method for estimating the BSSE. In the above equation, Counterpoise Method (CP) [27] was defined as an approximate method for estimating the BSSE. Detailed information about the BSSE correction has also been described in our previous studies [11-16]. Details are given in Ref. 16.

The nature of the interactions between CNTs and the IMQ drug, and the topological parameters, were determined from QTAIM which was employed with MULTIWFN 3.7 program [28].

This program creates RDG distribution plots against the Hessian electron density matrix with the second-largest eigenvalues. Scattering spots of RDG were drawn with the Gnuplot program [29]. The colour maps of their surfaces were visualised using the Virtual Molecular Dynamics (VMD) package [30].

3. Results and Discussions

All of the calculations, including geometry optimisation and single-point energy calculations, were performed by the Gaussian 09 package [25] as mentioned above in our previous study [11].

Adsorption Energies of IMQ molecule/CNTs

The results for the distance d(Å) between the Si-CNTs and IMQ molecule, the calculated adsorption energies (E_{ads}) and the transferred charge from IMQ drug to Si-CNT in the gas phase, are listed in Table 1.

Table 1. The distance d(Å), the Adsorption energies, Eads (Kj/mol) and the transferred charge of NTs, $Q(e)_{NT}$ in the gas phase.

Structure	d (Å)	E_{ads} (Kj/mol)	$Q(e)_{NT}$
IMQ/Si-CNTs			
N_4 /complex-A	1.980	-27.058	-0.316
N_2 /complex-B	1.891	-87.015	-0.331
N_3 /complex-C	1.907	-91.609	-0.332

The amount of charge transferred (CT) can be used as an indicator of the adsorption strength between the IMQ drug and Si-CNT for complexations.

The amount of CT from IMQ to Si-CNT in complex-A, complex-B, complex-C, and complex-D is -0.316, -0.331, -0.332, and -0.316e, respectively.

The adsorption energy values are in the following order: complex-C > complex-B > complex-D > complex-A.

The adsorption process can be classified based on the the E_{ads} values as physisorption or chemisorption. Interaction energies < 1 eV are known as physisorption [11]; otherwise, there is a strong interaction between the drug and Si-SWCNTs, indicating chemisorption. Thus, a more stable system corresponds to the more negative system. The adsorption energy must be negative for drug sensors and drug delivery devices. However, the lower-energy interaction process should be considered for drug sensor devices; a strong interaction corresponds to drug-delivery devices.

Topology Analysis of IMQ drug for N→Si Dative bonds using: Quantum Theory of Atoms in Molecules (QTAIM)

The concept of chemical bonding between the surfaces of NTs and components can be explained using topological analysis methods. Bader's theory of QTAIM is one of the best [23]. The electron density and bonding properties of IMQ/Si-SWCNTs complexes were investigated using the QTAIM methodology in the MULTIWFN program [28]. The nature of the interactions and bonds between the studied nanotubes and the drug, based on the electron density analysis, was obtained at the positions of (3, -1), which are called bond critical points (BCPs) because they usually appear between interacting atom pairs.

The computed molecular topographical map of selected complex structures given in Table 1 has been illustrated in Fig. 1, where orange balls exhibit the bond critical points of (3, -1). The cages and ring critical points correspond to green and yellow circles, and the lines represent bond paths.

(a)N_2/ complex-B

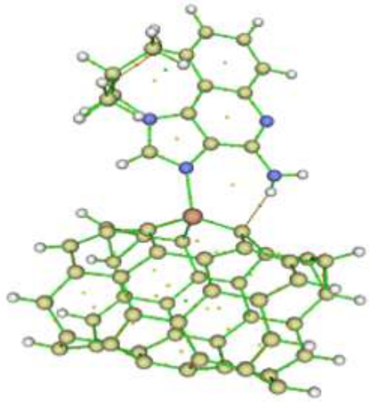

(b)N_3/ complex-C

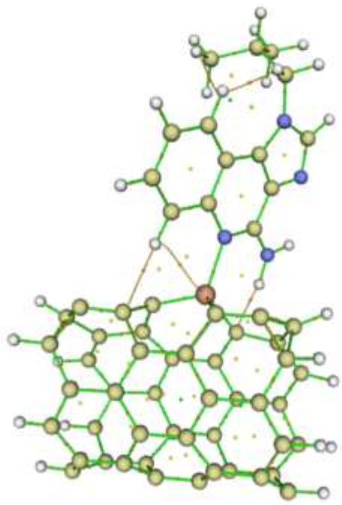

Fig.1. The topographical map of selected complexes for a) N_2-complex-B and b) N_3-complex-C.

The topology parameters are as follows: the electron density of $\rho(r)$, Laplacian $\nabla^2\rho(r)$, the total energy density of H(r), the Lagrangian kinetic energy of G(r), potential energy density of V(r) and, the ratio of $|V(r)|/G(r)$. In our discussion of the nature of the bonds formed by the interaction of the atoms of the Si-CNT and IMQ, the topology parameters were analysed and given in Table 2

Three bonding regimes, depending on the value of $|V(r)|/G(r)$ are distinguished by Bianchi et al. [31].

There are three characteristics of bondings: the intermediate bond regime $\nabla^2\rho(r) > 0, H(r) <$

0, and $1 < |V(r)|/G(r) < 2$, the electron shared covalent bonds if $H(r) < 0$, $\nabla^2\rho(r) < 0, |V(r)|/G(r) > 2$, and closed shell ionic bonds or the Van der Waals interactions /weak hydrogen bonding, if $H(r) > 0$, $\nabla^2\rho(r) > 0$, $|V(r)|/G(r) < 1$.

Table 2. The QTAIM topological parameters of the IMQ-Si-CNTs adsorbed compounds

Comp.	BCPs Drug/NT	ρ_{BCP}	$\nabla^2\rho_{BCP}$	G_{BCP}
A **N4-Si**	N61-Si36	0.072370	0.235221	0.083051
B **N_2-Si**	N61-Si36	0.084329	0.351223	0.113845
C **N_3-Si**	N61-Si36	0.261221	-0.61668	0.066084
		V_{BCP}	H_{BCP}	$\lvert H_{BCP}\rvert / \rho_{BCP}$
A **N_4-Si**	N61-Si36	-0.10729	-0.02424	0.3350
B **N_2-Si**	N61-Si36	-0.139884	-0.026039	0.3088
C **N_3-Si**	N61-Si36	-0.286338	-0.220254	0.8432

On the other hand, Macchi's classification [32] relies on the values of both local descriptors and the delocalization index and offers a way to refine bond characterization further.

In this study, we have focused on the N-Si dative bonds between the IMQ drug and Si-CNTs. For this reason, the covalence degree of dative bonds is estimated from the latter and from $H(r)/\rho(r)$, which is energy density per electron. Its value at BCP is due to the bond degree parameter (BD) [33]. Espinosa and co-workers [33] suggest that for covalent bonds (H_{BCP}<0) , the BD provides the degree of covalency and the stronger the interaction, the larger the BD magnitude; For closed shell interactions (H_{BCP}>0), BD can be viewed as the degree of softening and the weaker the interaction, the larger the BD magnitude. In the correlation scheme of Espinosa et al.[34], the strength of the interaction provides the corresponding positive interaction energy as given by E_{int}=$-V_{BCP}$*2 or the hydrogen bond energy (E_{HB}) rule, such as $E_{HB} = \frac{V_{BCP}}{2}$.

Dative Bond

A dative bond is a type of chemical bond where one atom provides a shared pair of electrons for bond formation, also called a Coordinate Covalent bond. The dative bond (DB) can be referred to as a coordinate covalent or donor-acceptor bond, and it shows similarities to a covalent bond because it involves an electron pair facilitating the bonding process Descriptors of dative bonds, such as bond ionicity and covalency, are important for accurate characterisation.

Bond covalency and ionicity:

It is known that some covalent bonds contain ionic characteristics, and some ionic bonds are partially covalent. The descriptors of the dative bond, such as bond covalency and ionicity, are important to determine the accurate characterisation of the dative bond.

$$\%Bond\ ionicity = \left[1 - exp[-(0.25)(X_A - X_B)^2]\right] \times 100 \quad (2)$$

Where X_A and X_B are the electronegativity values of A and B elements, respectively. The electronegativity values of Si (1.8), Al(1.5), C(2.5), N (3.0), O(3.5), H(2.1) [35]. The per cent bond covalency in the Si-N dative bond is about %69.76, in the N-C dative bond is about % 93.94 and in the Al-N dative bond is about % 56.978. For Si-O , it is about %48.

N→Si Dative Bonds

In general, N-Si bonds are stable in molecules, but the bond strength and character vary depending on the structure of the complex in which the bond is located.

Formation of Si Dative (Coordinative) Bonds:

In Si-CNT, the Si atom placed in the carbon lattice is electron-poor. The nitrogen (N) containing a free electron pair in the drug molecule behaves like a Lewis type bond. The formation of N→Si Dative Bonds as follows:

a) The N atom in the drug molecule contains a lone pair (free electron pair).

b) The Si atom on the Si-CNT is more electrophilic than the carbon structure and requires electrons with empty 3p orbitals.

c)The N atom donates its lone pair of electrons to the Si atom:

d) This creates coordinate (dative) N→Si bonds. These bonds are covalent but directional and often reversible, which offers an advantage in drug delivery systems. For an N→Si dative bond to form, the drug molecule must have free lone-paired nitrogen.

Here, the coordinative covalent bond formed between N and Si emerges during IMQ adsorption on the Si-CNT nanotube. The value of the electron density at a bond critical point in IMQ adsorption on the Si-CNT nanotube. is indicative of the strength of the covalent contribution to the bonded interactions.

***The topology parameters contributions on the* N→Si bonds**

According to QTAIM theory, the larger electron densities mean there are much stronger non-covalent bonds, and the Laplacian of electron density is positive at the BCPs at the non-covalent bond.

If the values of $\nabla^2\rho(r)$ and H(r) are less than zero, the interaction is described as covalent; if the values of $\nabla^2\rho(r)$ are greater than zero and H(r) are less than zero, the interaction is described as partially covalent. If the values of $\nabla^2\rho(r)$ and H(r) are positive, the interaction is defined as non-covalent in nature.

In general, for shared (covalent) bonding, $\rho(r)>0.20$ au and for closed-shell interaction, $\rho(r)<0.10$ au.

Based on the values given in Table 2, we analyse the bonding character of the complexes.

We compare the bond densities in Table 2, ρ_{BCP} of the complexes with one another according to their bond strengths and covalent properties.

For complex A, ρ_{BCP} =0.072→weak-moderate interaction.

The value =0.084 for complex B is stronger than that of A.

The ρ_{BCP} =0.261 for complex C is very high, indicating a strong covalent bond. Thus, the order of bond density is as follows: ρ_{BCP} **(C)>** ρ_{BCP} **(B) >** ρ_{BCP} **(A)**

Interpretation of Bond types: The bond density of complex C is three times that of the others, indicating a strength equivalent to a chemical bond. We can analyse the Laplacian of the bond character values. For the A and B complexes, the values of $\nabla^2\rho_{BCP}$ are positive and closed shell character (ionic/electrostatic slightly covalent compound).

The negative $\nabla^2\rho_{BCP}$ (-0.617) shows fully covalent bonding. Negative $\nabla^2\rho_{BCP}$ means that electron density is concentrated in the bond region. The C complex has a qualitatively different bond type than the others.

For N-Si bonds, $H_{BCP}(r)$ is negative (mostly between -0.11 and -0.29 a.u). This indicates that the bond has partial covalent character; it is not purely a weak/van der Waals interaction. In Table 2, the values of the ratio of $|H_{BCP}|/\rho_{BCP}$ range are 0.30-0.34. These values correspond to semi-covalent (partial covalent) bonds. The ratio of $|H_{BCP}|/\rho_{BCP}$ is an indicator of covalence. Those values are 0.335 and 0.308 for complexes of A and B, respectively. They are semi-covalent, but the complex C ratio is 0.843, which is very close to the covalent bonding region. Above 0.8 is considered covalent bonding. In other words, complex C is fully covalent. Another ratio of $|V(r)|/G(r)$ is one of the strongest determinants of bond type. If the range of $V(r)/G(r)$ is between 1.23 and 1.28, it indicates a weak covalent or mixed ionic-covalent character. If it were fully covalent, it would approach 2. The value of 1.29 for complex A shows weak covalent/closed-shell character. The value of 1.23 for complex B indicates a more ionic/electrostatic character. The value 4.33 is typical for a covalent bond in complex C. Such a high value is typical for short, intense, fully covalent bonds.

E_{HB} Bond Energy and type of interactions: The bond energies calculated by $E_{HB} = \frac{V_{BCP}}{2}$ are listed in Table 3.

The most negative (i.e., lowest) binding energies, such as -372 kj/mol, indicate high values. Such high binding energies are generally suitable for permanent binding (e.g., drug carriers). Lower binding energies (e.g., -74 kJ/mol or -140 kJ/mol) usually allow for temporary, reversible binding and thus easier release for delivery.

Table 3. The E_{HB} energy, bonding character of the IMQ-Si-CNTs adsorbed compounds

Comp.	BCPs Drug/NT	**E_{HB} (kJ/mol)**	Ni→Si Dative Bonds	π-π Interac.
A **N4-Si**	N61-Si36	-139	Strong	Weak-moderate
B **N2-Si**	N61-Si36	-182	Very Strong	Medium
C **N3-Si**	N61-Si36	-372	Extremely powerful	Medium
		Vander Waals (Dispers.)	General comment on bond	
A **N4-Si**	N61-Si36	Medium	Dative bond prominent	
B **N2-Si**	N61-Si36	Strong	Dative bond + dispersion	
C **N3-Si**	N61-Si36	Extreme Dispers.	Most stable complex	

The degree of N-Si dative bonds, as well as π-π and van der Waals interactions, is also analysed.

The degree of N-Si bonds is described as follows: For complex A, it is an N-Si coordinative bond where electrostatic interactions are predominant.

For complex B, the length of the N-Si bonds is shorter than that of complex A (1.891). $H_{BCP}(r)$ is more negative than the complex A, thus its covalent contribution is increased. Still, it is a closed shell + partial covalent bond. It exhibits stronger coordination than complex A.

For complex C, all indicators suggest a covalent N-Si bond.

The negative Laplacian indicates electron accumulation in the bond region. Furthermore, complex C is qualitatively entirely different from the others. This bond is not a classical coordination interaction but an actual N-Si bond.

Based on the results listed in Tables 1-3, if the Laplacian is positive and $H_{BCP}(r)$ is less negative, these bonds may be weak or ionic in character and more transient bonds.

Particularly, some bonds in complexes A and B are weaker and have an ionic character. Thus, the NCI analysis must have needed those complexes.

The Non-Covalent Interactions(NCI) Analysis /Reduced Gradient Density (RDG)

The analysis of reduced density gradient (RDG) and non-covalent interactions (NCI) is a valuable method based on the system's electron density. The RDG function can be calculated as follows

$$RDG(\boldsymbol{r}) = \frac{1}{2\,(3\pi^2)^{1/3}} \frac{|\Delta\rho(\mathbf{r})|}{\rho(\boldsymbol{r})^{4/3}} \tag{3}$$

where $\boldsymbol{r}$ is a coordinate vector and ρ represents electron density. The bond strengths are determined from $\rho(\boldsymbol{r})$ values. Moreover, the regions of the graphs for each specific RDG value can be classified in three ways based on the sign of (sign λ2) ρ(r), which means that the sign of the second largest eigenvalue of the electron density Hessian matrix at position r. To perform the RDG analysis, we have used the Multiwfn 3.7 software package [28]. The selected complex with the weak adsorption energy given in Table 1 as complex A was plotted of RDG versus (sign λ2) ρ(r) in Fig.2.

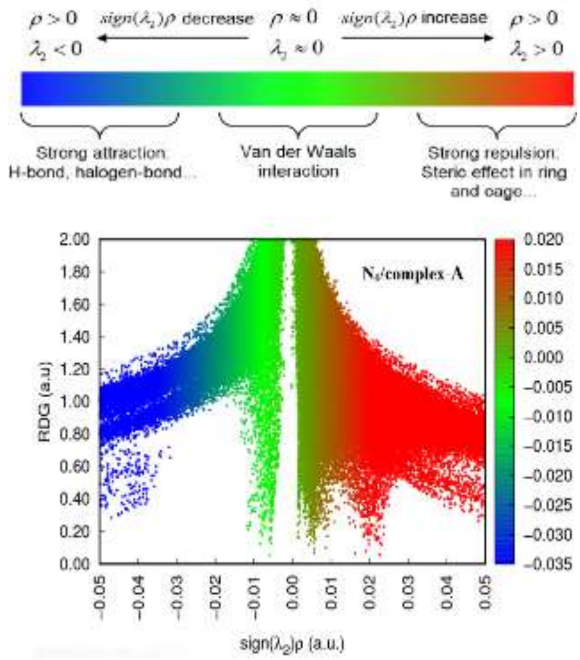

Fig 2. RDG scatter plots for N_4 /complex-A

This means there are strong repulsion interactions, weak van der Waals interactions, and strong attraction. It is displayed in red, green, and blue colours based on the (signλ2) ρ value. Strong electrostatic interactions, van der Waals forces, and repulsion are shown in blue, green, and red colours, respectively. Weak interactions are analysed with NCI plots. This graph is an NCI analysis graph showing the relationship between RDG and (sign λ2) ρ(r), which determines the type of interaction in complex-A.

On the right side of the graph in Fig. 2, a dense data distribution is observed in the red region, where spikes for N_4/complex-A are present. This indicates that there are significant steric repulsive or repulsive interactions in the N_4/complex-A system.

The green region in Fig2. as ((sign λ2) ρ(r)≈0), shows Van der Waals interactions. The areas shown in green-blue tones in the middle indicate weak van der Waals interactions. The blue region (sign (λ2) ρ(r) < 0, negative) exhibits attractive interactions. The blue-green areas on the left indicate hydrogen bonding or other attractive interactions, respectively, but the blue region is less intense than the red region. The RDG isosurfaces for IMQ/Si-CNTs obtained from VMD [30] are shown in Fig3.

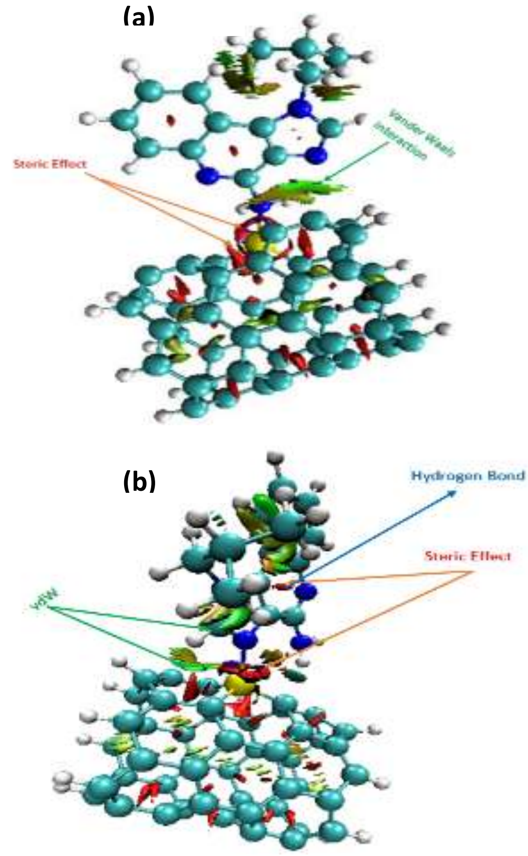

Fig 3. 3-D Graphics of RDG iso surfaces for a) N_4 /complex-A and b) N_2 /complex-B

The isosurfaces of sign (λ2) obtained for the N_4 /complex-A and N_2/complex-B are depicted and colour coded accordingly in Fig. 3a-b, respectively.

In Figs. 3a and 3b: the red circles between the Si-CNT and IMQ drug indicate steric interactions within the IMQ/Si-CNT complexes. The green oval circles between the Si-CNTs and the IMQ drug indicate vdW interactions between the systems.

The interaction indicated by the blue arrow in Fig. 3b usually occurs between a hydrogen atom (N-H or O-H) and an electronegative atom (such as O and N). It is weaker than a covalent bond but stronger than vdW interactions. It is known that the hydrogen bonds provide directionality and specificity. However, in this study, we focus on the N-Si bonds, namely steric and vdW interactions between the Si-CNT and the IMQ drug in the drug delivery and drug carrier. Steric effects determine which conformation is possible. Physically prevents incorrect bindings. The vdW interactions contribute to the total binding energy. When considered together, we can say that the binding in both complexes is achieved with a stable but flexible equilibrium. The steric influence prevents incorrect positions, and binding energy is maximised through vdW interactions.

Drug Carrier and Drug Delivery

Drug carrier cases where the drug is strongly and stably bound to the nanotube. In this case, the drug remains on the surface and is generally used for controlled release.

Drug Delivery cases where the drug is weak and has temporary bonds. Such bonds are suitable for the easy transport and release of the drug from the nanotube into the target region and are used for drug delivery.

For each N-Si bond listed in the Tables, we can categorise the bond type and potential application (drug carrier or drug delivery) as follows:

Based on Tables 2 and 3, complexes with strong bonds, especially N_3/complex-C, can be regarded as drug carriers. Drug release might be challenging for this type of complex structure. Its use is limited to drug delivery.

For an ideal drug carrier, Si-CNTs should securely contain the drug while allowing controlled release. N_4 /complex-A has low Eads and physical adsorption. It is the most suitable drug carrier and offers advantages for controlled release. N_2 /complex-B has medium-high Eads. It is suitable for controlled release systems with Transport and partial strong retention. Evaluation from a drug sensor perspective: It requires strong binding and high charge transfer for an effective sensor. The top sensor candidates among the studied complexes are as follows:

N_3/complex-C produces the maximum signal, indicating high sensitivity; N_2/complex-B shows balanced sensor performance; N_4/complex-A results in a weaker sensor response. Additionally, Si-CNTs can be regarded as multifunctional nanoplatforms for IMQ drug delivery. For N_2/complex-B and N_4/complex-A, Si-CNTs are suitable for controlled drug delivery and release, whereas for N_3/complex-C, Si-CNTs are notable as high-sensitivity IMQ sensors. The sensitivity ranking for drug sensors is as follows: N_3/complex-C > N_2/complex-B > N_4/complex-A.

The significance of N-Si dative bonds in drug delivery, sensing, and detection applications:

Weak N-Si dative bonds are temporary and reversible, allowing the drug to adhere to the surface and then be released. This process is crucial in drug delivery systems, where the drug is released upon reaching the target. Medium-strength N-Si dative bonds are more stable but still not completely unbreakable. They provide stability during transport and enable controlled release, making them suitable for both drug delivery and carrier systems. Strong covalent N-Si dative bonds, as seen in complex-C, are a form of robust coordinative covalent dative bond with covalent character. This strong dative bond results from the direct coordination of electron pairs from N to Si and is the most suitable bond type for drug carriers. These bonds permit the drug molecule to attach to the Si-CNT surface, and the bond strength and nature affect the system's function.

3. Conclusion

This study attempted to explain the adsorption, interaction, of IMQ on Si-CNT using DFT M062X/ 6-31G (d) in the gas phase. The obtained data showed that the drug was active in forming dative bonds, as indicated by dative bond parameters, and in adhering to nanotubes.

In conclusion, according to the results, N-Si bonds differ structurally and electronically in different complexes. Some bonds (e.g., complex-C) are covalent and quite strong. In general, N-Si bonds are stable in molecules, but the bond strength and character vary depending on the structure of the complex in which the bond is located.

If the bond strength is high (very negative energy, short bond length, high electron density), the system functions as a drug carrier. If the bond strength is relatively low and the interactions are weak, the nanotube can be used for drug delivery. Complexes with the strongest bonds in the table indicate that the nanotube acts as a carrier by firmly binding the drug; other weaker bonds mean that the nanotube can deliver and release the drug to the target.

Therefore, according to results given in the tables, there are different complexes that exhibit both drug-carrier and drug-delivery potential. The binding character will be critical depending on the specific use.

This study demonstrates that Si-CNTs can be used as multifunctional nanostructures for IMQ drug delivery, depending on the type of N-atom binding. Accordingly, both

N_4/complex-A and N_2/complex-B will display weak ionic bonds, aiding drug delivery. They are suitable for drug delivery and controlled release applications. The N_3/complex-C will form a strong covalent bond, ensuring permanent attachment to the drug carrier. The N_3/complex-C system is particularly notable as a highly sensitive drug sensor for detecting IMQ drugs.

In conclusion, the N-Si coordinative bond is not only a fundamental bonding mode that controls the electronic and chemical properties of Si-CNTs; it is also a decisive theoretical element in targeted drug delivery, nanosensor design, and the rational design of functional carbon nanomaterials.

Therefore, investigating the N-Si bond at the atomic level is indispensable, both theoretically and practically, for understanding and optimizing Si-CNT-based nanotechnologies.

References

[1] J. K. Patra, G. Das, L. F. Fraceto, E. V. R. Campos, M. P. Rodriguez-Torres, et al, Nano-based drug delivery systems and future prospects, J. Nanobiotechnol. , 16(1) (2018) 71. https://doi.org/10.1186/s12951-018-0392-8

[2] A. R. Mashweu, V. A. Azov, Nanotechnology in Drug Delivery: Anatomy and Molecular Insight into the self-assembley of Peptide-Based Hydrogels, Molecules, 29 (2024) 5654. https://doi.org/10.3390/molecules29235654

[3] P. K. Gupta (2023), Nano-Based Drug Delivery Systems. In: Nanotoxicology in Nanomedicine: Chap. 6: , , Springer Press, ISBN 978-3-031-24286-1, https://doi.org/10.1007/978-3-031-24287-8_6

[4] Y. Huang, P. Li, R. Zhao, L. Zhao, J. Liu, S. Peng, X. Fu, X. Wang, R. Luo, R. Wang, Z. Zhang, Silica nanoparticles: Biomedical applications and toxicity,151 (2022)113053. https://doi.org/10.1016/j.biopha.2022.113053

[5] K. S. Ibrahim, Carbon nanotubes-properties and applications: a review, Carbon Lett. 14(3) (2013) 131. https://doi.org/10.5714/CL.2013.14.3.131

[6] M. A. Saleemi, Y. L. Kong, P. V. C. Yong, E. H. Wong, An overview of recent development in therapeutic drug carrier system using carbon nanotubes, J. Drug Delivery Science and Technology, 59 (2020) 101855-101865. https://doi.org/10.1016/j.jddst.2020.101855

[7] K. Sushma, G. Surendra, Om. M. Bagade, P. Jahnavi, A. Averineni, S. Rani, V. Kiran, P. S. Gupta, Metallic Nano carriers for Targeted Delivery of Anticancer Drugs: Advances and Therapeutic Potential, J. Appl. Organomet. Chem., 5(4) (2025) 508. https://doi.org/10.48309/JAOC.2025.534798.1315

[8] M. Sargolzaei, M. Afshar, H. Nikoofard, Solvent Effect on The Equilibrium and Rate Constant of the Tautomeric Reaction in Nexium, Skelaxin, Aldara and Efavirenz Drugs: A DFT Study. Journal of Structural Chemistry, 59 (2018) 297-305. https://doi.org/10.1134/S0022476618020063

[9] S. Mahajan, A. Patharkar, K. Kuche, R. Maheshwari, P. K. Deb, K. Kalia, R. K. Tekade, Functionalized carbon nanotubes as emerging delivery system for the treatment of cancer, International J. Pharmaceutics, 548(1) (2018) 540-558. https://doi.org/10.1016/j.ijpharm.2018.07.027

[10] H. Yan, Z. Xue, J. Xie, Y. Dong, Z. Ma, X. Sun, D. K. Borga, Z. Liu, J. Li, Toxicity of Carbon Nanotubes as Anti-Tumour Drug Carriers, Int. J. Nanomedicine 14 (2019) 10179-10194. https://doi.org/10.2147%2FIJN.S220087

[11] S. Senturk Dalgic, Dilek Kuzalic Burucu, S. Dalgic, F. Kandemirli, A comparative DFT study on the interaction of Aldara drug molecule with SiC and Si-carbon nanotubes, J. Appl. Phys., **137** (2025) 135104. https://doi.org/10.1063/5.0255569

[12] H. S. Sayiner, F. Kandemirli, S. Senturk Dalgic, M. Monajjemi, F. Mollaamin, Carbazochrome carbon nanotube as drug delivery nanocarrier for anti-bleeding drug: quantum chemical study, J. Mol. Modelling, 28 (2022) 11. https://doi.org/10.1007/s00894-021-04948-1

[13] Z. Al-Sawaff, S. Senturk Dalgic, F. Kandemirli, Theoretical study of the adsorption of BMSF-BENZ drug for osteoporosis disease treatment on Al-doped carbon nanotubes (Al-CNT) as a drug delivery vehicle, European Journal of Chemistry, 12(3) (2021) 314. https://doi.org/10.5155/eurjchem.12.3.314-322.2143.

[14] Z. Al-Sawaff, S. Senturk Dalgic, F. Kandemirli, M. Monajjemi, F. Mollaamin, DFT Study Adsorption of Hydroxychloroquine for Treatment COVID-19 by SiC Nanotube and Al, Si Doping on Carbon Nanotube Surface: A Drug Delivery Simulation, Russ. J. Phys. Chem., 96, (2022) 2953. https://doi.org/10.1134/S003602442213026X

[15] Z. H. Al-Sawaff, S. Senturk Dalgic, F. Kandemirli, Density Functional Theory (DFT) Study on Silicon Doped Carbon Nanotube Si-CNT as a Carrier for BMSF-BENZ Drug used for Osteoporosis Disease, MOMENTO, 65 (2022) 1. https://doi.org/10.15446/mo.n65.99010

[16] S. Senturk Dalgic, Z. H. Al-Sawaff, S. Dalgic, F. Kandemirli, A comparative DFT study on Al- and Si-doped single wall carbon nanotubes (SWCNTs) for Ribavirin drug sensing and detection, Material Science in Semiconductor Process. 158 (2023) 107360. https://doi.org/10.1016/j.mssp.2023.107360

[17] S. Mahajan, A. Patharkar, K. Kuche, R. Maheshwari, P. K. Deb, K. Kalia, R. K. Tekade, Functionalized carbon nanotubes as emerging delivery system for the treatment of cancer, International J. Pharmaceutics, 548(1) (2018) 540. https://doi.org/10.1016/j.ijpharm.2018.07.027

[18] H. Alinezhad, M. D. Ganji, E. Soleymani, M. Tajbakhsh, A comprehensive theoretical investigation about the bio-functionalization capability of single-walled CNT, BNNT and SiCNT using DNA/RNA nucleobases, Applied

Surface Science 422 (2017) 56. https://doi.org/10.1016/j.apsusc.2017.05.196

[19] F. Kandemirli, S. Senturk Dalgic, Computational study of SiCNT interacting with Benidipine, J. mater. electron. device. 4 (2024) 1.

[20] A. Nandi, S. Kozuch, History and Future of Dative Bonds, Chem. Eur. J. 26 (2020) 759. https://doi.org/10.1002/chem.201903736

[21] I. V. Strekhova, A. A. Korlyukov, N. F. Lazerava, V. I. Smirnov, Silatranes: Relationship between the experimental Si-N dative bond length and its calculated energy according to AIM analysis data, Chem. Phys., 578 (2024) 112153. https://doi.org/10.1016/j.chemphys.2023.112153

[22] R. Lo, D. Manna, V. M. Miriyala, D. Nachtigallova, P. Hobza, Trends in the stability of covalent dative bonds with variable solvent polarity depend on the charge transfer in the Lewis electron-pair system, Phys. Chem. Chem. Phys. , 25 (2023) 25961. https://doi.org/10.1039/D3CP03445C

[23] R.F.W. Bader, Atoms in molecules, Acc. Chem. Res. 18 (1985) 9–15, https://doi.org/10.1021/ar00109a003

[24] E. R. Johnson, S. Keinan, P. Mori-Sanchez, J. Contreras-Garcia, A. J. Cohen, W. Yang, Revealing noncovalent interactions, J. Am. Chem. Soc., 132(18) (2010) 6498. https://doi.org/10.1021/ja100936w

[25] Gaussian 09 Revision B.01, D.J.F. M. J. Frisch, G. W. Trucks, H. B. Schlegel, G. E. Scuseria, M. A. Robb, J. R. Cheeseman, G. Scalmani, V. Barone, B. Mennucci, G. A. Petersson, H. Nakatsuji, M. Caricato, X. Li, H. P. Hratchian, A. F. Izmaylov, J. Bloino, G. Zheng, J. L. Sonnenberg, M. Had, M.J. Frisch, G.W. Trucks, H.B. Schlegel, G.E. Scuseria, M.A. Robb, J.R. Cheeseman, G. Scalmani, V. Barone, B. Mennucci, G.A. Petersson, H. Nakatsuji, M. Caricato, X. Li, H.P. Hratchian, A.F. Izmaylov, J. Bloino, G. Zheng, J. L. Sonnenberg, M. Hada, M. Ehara, K. Toyota, R. Fukuda, J. Hasegawa, M. Ishida, T. Nakajima, Y. Honda, O. Kitao, H. Nakai, T. Vreven, J.A. Montgomery Jr., J.E. Peralta, F. Ogliaro, M. Bearpark, J.J. Heyd, E. Brothers, K.N. Kudin, V.N. Staroverov, R. Kobayashi, J. Normand, K. Raghavachari, A. Rendell, J.C. Burant, S. S. Iyengar, J. Tomasi, M. Cossi, N. Rega, J.M. Millam, M. Klene, J.E. Knox, J.B. Cross, V. Bakken, C. Adamo, J. Jaramillo, R. Gomperts, R.E. Stratmann, O. Yazyev, A.J. Austin, R. Cammi, C. Pomelli, J.W. Ochterski, R.L. Martin, K. Morokuma, V.G. Zakrzewski, G.A. Voth, P. Salvador, J.J. Dannenberg, S. Dapprich, A.D. Daniels, ¨O. Farkas, J.B. Foresman, J. V Ortiz, J. Cioslowski, D.J. Fox, Gaussian 09, , Gaussian Inc., Wallingford. (2013). https://gaussian.com/glossary/g09/

[26] H. Moradnia, H. Raissi, A. Bakhtiari, A density functional theory-based analysis of the structural, topological and electronic properties of gemcitabine drug adsorption on the pyrrolidine functionalized single-walled carbon nanotube. J. Biomolecular Structure and Dynamics, 37 (2019) 2477. https://doi.org/10.1080/07391102.2018.1491892

[27] S.F. Boys, F. Bernardi, The calculation of small molecular interactions by the differences of separate total energies. Some procedures with reduced errors, Molecular Physics, 19 (1970) 553-566. https://doi.org/10.1080/00268977000101561

[28] T. Lu, F. Chen, Multiwfn: a multifunctional wave function analyser, J. Comput. Chem. 33 (2012) 580. https://doi.org/10.1002/jcc.22885

[29] W. Thomas, C. Kelley, Gnuplot 4.5: an Interactive Plotting Program, 2011. http://gnuplot.info

[30] W. Humphrey, A. Dalke, K. Schulten, VMD: visual molecular dynamics, J. Mol. Graph. 14 (1996) 33. https://doi.org/10.1016/0263-7855(96)00018-5

[31] R. Bianchi, G. Gervasio, D. Marabello. Experimental Electron Density Analysis of Mn2(CO)10: Metal-Metal and Metal-Ligand Bond Characterization, Inorg. Chem. 39, (2000) 2360. https://doi.org/10.1021/ic991316e

[32] P. Macchi, D.M. Proserpio, A. Sironi, Experimental Electron Density in a Transition Metal Dimer: Metal-Metal and Metal-Ligand Bonds, J. Am. Chem. Soc. 120 (1998) 13429. https://doi.org/10.1021/ja982903m

[33] E. Espinosa, I. Alkorta, J. Elguero, E. Molins, From weak to strong interactions: A comprehensive analysis of the topological and energetic properties of the electron density distribution involving X-H.... F-Y systems. J. Chem. Phys. 117 (2002) 5529. https://doi.org/10.1063/1.1501133

[34] E. Espinosa, E. Molins, C. Leconte, Hydrogen bond strengths revealed by topological analyses of experimentally observed electron densities, Chem. Phys. Lett. 286 (3–4) (1998) 170, https://doi.org/10.1016/S0009-2614(98)00036-0

[35] W. D. Callister, D.G. Rethwisch, Material Science and Engineering, 8th Edition, Wiley.

.